Molecular Dynamics Simulations of Surface Tensions of Aqueous Electrolytic Solutions

Divesh Bhatt, John Newman, and C. J. Radke*

Department of Chemical Engineering, University of California, Berkeley, California 94720-1462

Received: October 23, 2003; In Final Form: December 18, 2003

We present molecular-dynamics (MD) simulations of surface tension of aqueous ionic solutions of different concentrations for two different salts with different anion size: NaCl and NaF at 300 K in explicit water molecules. Our MD results agree quite closely with the experimental results. In particular, our MD results predict that the salt with a larger anion (NaCl) shows a smaller increase in surface tension than the salt with a smaller anion (NaF). To check the limits of applicability of the solvent primitive model (SPM), we solve exactly the system with the approximation that the solvent (water) is a background dielectric continuum using MD simulations. Compared with explicit water MD simulations, SPM gives qualitatively incorrect results for the dependence of surface tension on the type of salt. More precisely, with the solvent as a dielectric continuum, an NaCl solution shows a larger increase in surface tension than does an NaF solution. Strong water structuring around the solvated ions is the proposed explanation.

Introduction

It is well established experimentally that most inorganic salts increase the surface tension of water.[1] The earliest theoretical work addressing this issue dealt purely with electrostatic interactions between ions of the dissociated dissolved electrolyte with the solvent as a dielectric medium and did indeed show the qualitative trend of an increase in surface tension over the surface tension of pure water.[2] However, because only electrostatics was considered, all salts containing the same charge on the ions (e.g., 1:1 or 1:2 electrolytes) showed the same surface-tension behavior in the theoretical developments.

Recently, a significant amount of work has been done to understand theoretically the role of ion specificity on the surface tension of electrolyte solutions,[3−6] or, in broader terms, to understand the so-called Hofmeister series.[7] This problem is related to the role of ion specificity in protein, micellar, and polyelectrolyte solutions. A basic idea in these treatments is that ion specificity can be accounted for by considering dispersion interactions between ions and across the interface that are different for different types of ions,[4,5] while still treating water as a dielectric continuum. The specific dispersion interaction that each ion has with the interface (modeled as a dielectric discontinuity) leads to the possibility of charge separation at the interface and, hence, an electrostatic field to counter that charge separation. The distribution of each type of ion away from the interface is treated by the Boltzmann distribution, which consists of three separate terms: the usual electrostatic potential, the ion-specific dispersion interaction as mentioned above, and a non-ion specific image potential due to the dielectric discontinuity at the interface.[4,5] To obtain the electrostatic potential, and thus, the distribution of ions from the interface, Poisson's equation is solved with the above given Boltzmann distribution. This approach is called the modified Poisson−Boltzmann (MPB) model. The ion density profile calculated from MPB, along with the Gibbs adsorption equation,[8] then gives the surface tension as a function of salt concentration.

Several important issues arise in the MPB treatment. One is the choice of parameters for the different types of ions. An important question is whether the parameters can be determined a priori or are fitting parameters whose physical interpretation is not clear. Dispersion interactions between ions and the interface scale with the inverse cube of the distance from the interface and are typically characterized by an ion-dependent dispersion coefficient B_i.[4,5] A larger positive value of B_i results in the ion being more repelled from the interface, and gives a larger increase in surface tension. To fit the experimental surface-tension results, for example, F^- must have a larger positive value of B_i than does Cl^-, which in turn must be larger than B_{Br^-}.[4] On the other hand, the physical picture of the ion-surface dispersion coefficients is that an ion with the highest electron density (Br^-, for the above example) has the largest value of B_i. This apparent contradiction between expected values of the ion-surface dispersion coefficients and those obtained from empirical fits to the experimental data is of fundamental importance in understanding the effect of ion specificity on the surface properties of electrolyte solutions and on the Hofmeister series in general.

Another major approximation used in MPB is, of course, the treatment of water as a dielectric continuum. Thus, MPB neglects water structure around ions that is different for different types of ions, as shown in previous simulations of aqueous ionic solutions.[9−11] Still another approximation of the MPB model is the neglect of specific interactions between ions in the solution. At high concentrations, when electrostatic forces are screened, the neglect of ion−ion specific interactions is expected to be severe. Additionally, the salt chemical potentials needed to calculate the increase in surface tension over that of pure water are determined from actual experimental data. These chemical-potential values may not necessarily correspond to the potentials used to calculate the negative excess adsorption in MPB. Possibly the incorporation of ion−ion interactions and consistent salt chemical potential, while still treating water as a background dielectric to maintain simplicity, may resolve the inconsistency in B_i values mentioned above.

In this work, we address the above questions. First, we obtain exact surface-tension results for given ionic-potential models

* Author to whom correspondence should be addressed. Phone: 510-642-5204. Fax: 510-642-4778. E-mail: radke@cchem.berkeley.edu.

10.1021/jp037212d CCC: $27.50
Published on Web 06/02/2004

by use of molecular-dynamics (MD) simulations with explicit water molecules. As described later, ionic-potential models are chosen for two salts with the same cation but different anions, NaCl and Na"F" (we discuss the reason for placing quotation marks around F shortly), and we compare our simulation results to experiment. Even without comparison to experiment, MD gives exact results for the potential models adopted and, thus, serves as a benchmark against which theories that use the same potential models can be compared. Thus, we use the same ionic-potential models to solve "exactly" the model in which water is a dielectric medium (the so-called solvent primitive model, SPM). Exact solution of ions in SPM is again provided by MD (with water not explicit, but characterized by a constant dielectric permittivity), with the same ionic potentials as those used in the explicit-water MD. This exercise answers the question of whether a more rigorous solution of MPB (still within the SPM) results in a better match with MD that adopts explicit water molecules.

It is known that the F^- anion reacts with water to produce HF_2^- and OH^- anions.[12] From the free energy of formation of the species in this reaction,[13] the equilibrium ΔG for this reaction at 300 K is calculated as -13.365 kJ/mol. Accordingly, in an aqueous NaF solution, the concentration of HF_2^- is even larger than that of F^-. A MD simulation with explicit water molecules that utilizes only the ionic-potential models for Na^+ and F^- is, therefore, not expected to represent an experimental NaF solution quantitatively. We denote our MD sodium fluoride aqueous solution (that considers only F^- anions) as Na"F" to distinguish it from an actual experimental NaF solution. Any comparison of the MD specific Na"F" solution with experimental NaF solutions is strictly qualitative. Nevertheless, as mentioned above, a comparison of explicit water MD simulation of Na"F" with that of Na"F" in the SPM is still valid quantitatively.

Electrolyte Solutions with Explicit Water

Simulation Details. The intermolecular-potential model we choose for simulating water is the extended simple-point-charge (SPC/E) model of Berendsen et al.[14] In this model, the potential energy between two water molecules i and j is

$$u_{ij} = 4\epsilon_{oo}\left[\left(\frac{\sigma_{oo}}{r_{io,jo}}\right)^{12} - \left(\frac{\sigma_{oo}}{r_{io,jo}}\right)^{6}\right] + \frac{1}{4\pi\epsilon_0}\sum_{a=1}^{3}\sum_{b=1}^{3}\frac{q_{ia}q_{jb}}{r_{ia,jb}} \quad (1)$$

where ϵ_{oo} and σ_{oo} are, respectively, the Lennard-Jones (LJ) energy and size parameters for the oxygen atoms in each water molecule, $r_{ia,jb}$ is the distance between atom a ($a = 1$ and 3 for hydrogen atoms, and $a = 2$ for oxygen) of molecule i and atom b of molecule j, ϵ_0 is the permittivity of free space, and q_{ia} is the (partial) charge on atom a of molecule i. In the SPC/E model of Berendsen et al.,[14] $\epsilon_{oo} = 650.2$ J/mol and $\sigma_{oo} = 0.3166$ nm. In addition, the partial charge on each oxygen site is $q_{io} = 0.8476q_e$, and on each hydrogen site is $|q_{io}|/2$, where q_e is the charge of an electron.

Ions also interact with one another and also with each atom of the water molecules with a coulombic as well as an LJ part. In this work, the ions chosen are Na^+ ($\epsilon_{Na^+,Na^+} = 142.17$ J/mol, $\sigma_{Na^+,Na^+} = 0.258$ nm),[15] Cl^- ($\epsilon_{Cl^-\ Cl^-} = 215.33$ J/mol, $\sigma_{Cl^-,Cl^-} = 0.462$ nm),[15] and F^- ($\epsilon_{F^-,F^-} = 50.0$ J/mol, $\sigma_{F^-,F^-} = 0.40$ nm).[11,16] For two different types of ions, i and j, the interactions are modeled by $\epsilon_{i,j} = \sqrt{\epsilon_i\epsilon_j}$ and $\sigma_{i,j} = \sqrt{\sigma_i\sigma_j}$. Additionally, the magnitude of charge on each ion is $|q_e|$. The above potential models for NaCl, along with SPC/E water, give a reasonable estimate of aqueous salt properties such as the activity and diffusion coefficients.[15]

Liquid-film slabs surrounded by vapor space are symmetrically placed in the simulation box and simulated with canonical-ensemble MD using the Nose-Hoover thermostat,[17−20] with periodic boundary conditions. Long-range coloumbic interactions are evaluated using the Ewald summation method.[21,22] In addition, instead of adding tail corrections, we use an Ewald-like technique to calculate the LJ part of the interaction.[22,23] For computational efficiency, this necessitates the use of the geometric mean for $\sigma_{i,j}$, instead of the more usual arithmetic mean. The parameters for Ewald summation were calculated from the method in reference 22 as given elsewhere.[24]

The number of water molecules is fixed at 534, and the salt (either NaCl or Na"F" in a particular simulation) concentration is varied, whereas the simulation temperature is fixed at $T = 300$ K. The x and y edge-lengths of the simulation box, L_x and L_y, are 2 nm each, while the z edge length, L_z, is 10 nm. Alejandre et al.[25] have established that the thermodynamic properties, such as the coexistence densities and the surface tension, of systems of this size are independent of system size. Equilibrium properties are averaged for about 1 ns (except the lowest Na"F" and the highest NaCl concentration that are averaged for 2 ns) after an initial equilibration period of 100 ps.

We evaluate the normal (zz) and the tangential (xx and yy) components of the Irving and Kirkwood (IK) pressure tensor,[25−29] and the surface tension is obtained from the expression[25]

$$\gamma = \frac{L_z}{2}\left\langle p_{zz} - \frac{1}{2}(p_{xx} + p_{yy})\right\rangle \quad (2)$$

where p_{ii} is the ii component of the pressure tensor.

Surface-Tension Results. For pure water at 300 K, we obtained $\gamma = 70.1 \pm 1.4$ mN/m, which agrees well with both the experimental result and the previous simulations for SPC/E water that employed a tail correction for the LJ potential beyond the cutoff.[25,29] These results validate our simulation, and show that by treating the LJ part of the interaction by an Ewald-type summation, we are considering the whole LJ interaction without the need for a tail correction.

Figures 1 (a) to (c) show the water and ionic-density profiles (in g/cm^3 and molar, respectively) for three different NaCl concentrations where the number of cations and anions each range from 20 to 60 (the number of water molecules is 534). Similarly, Figures 1 (d) to (f) are for three different Na"F" concentrations with the number of cations (and anions) ranging from 20 to 60, as shown labeled in the graphs. All the ionic-density profiles reach a plateau value in the center of the film, except those in Figure 1 (f), perhaps, due to insufficient averaging. For each salt, the ions are preferentially excluded from the vicinity of the water/vapor interface. A similar behavior is seen for ions near molecular hydrophobic solutes.[30] The distance of exclusion corresponds to about the size of a water molecule, implying that the ions (with the chosen potential model) tend to remain hydrated near the interface for the range of concentration studied. Moreover, as the salt concentration is increased (from (a) to (c), or from (d) to (f)), the ion density profiles exhibit a distinct peak. The peak arises because the ions behave as hydrated hard spheres that are excluded from the interface (in a manner analogous to the radial distribution in a liquid). Moreover, it is obvious from the figure that both the cationic and the anionic density profiles are almost the same, implying that the local charge separation is small. However, we note that the above observations are only for the particular

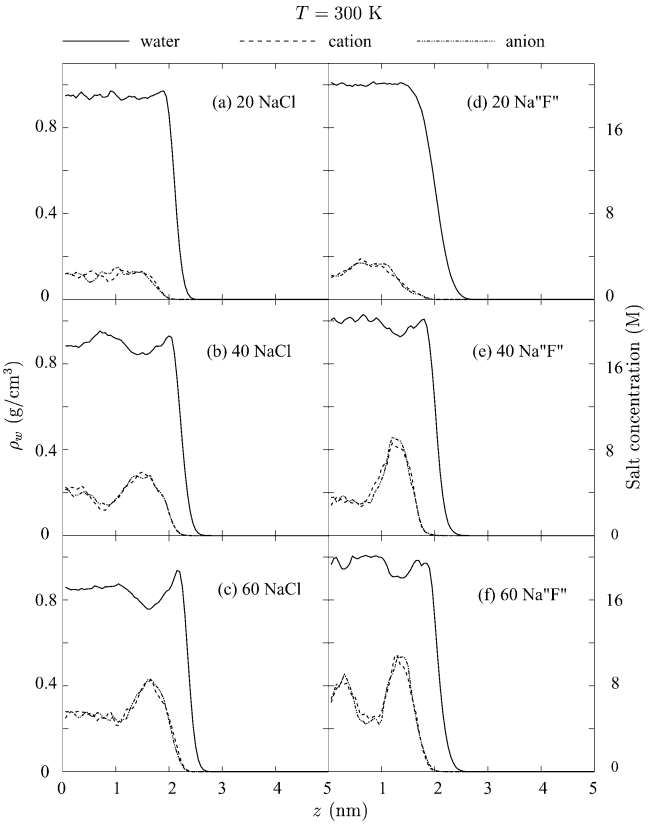

Figure 1. Water (in g/cm^3) and ionic density (in M) profiles for NaCl in (a) to (c), and for Na"F" in (d) to (f) at 300 K. The number of salt molecules simulated is listed in each figure panel. For all the concentrations simulated, the number of water molecules is 534.

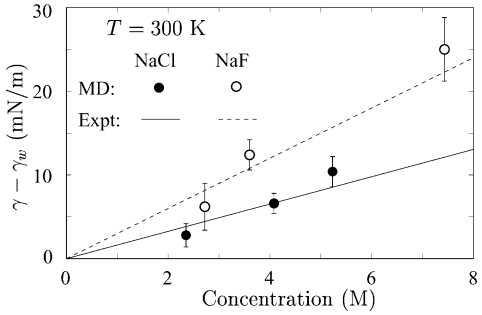

Figure 2. Surface tension relative to that of pure water as a function of salt concentration. The lines represent the experimental data; the symbols represent the MD results.

potential models (for water and ions) chosen. Recently, Jungwirth and Tobias[31] used a polarizable-potential model for a series of sodium halide salts and water and observed that the cationic and anionic density profiles for NaCl at 1.2 M show some charge separation with the Cl^- ion residing closer to the interface. Nevertheless, our results are in accord with previous works that used nonpolarizable single-ion density distributions near an interface.[32,33]

Figure 2 plots the surface tension of NaCl and Na"F" solutions, γ, minus that of pure water, γ_w. Closed circles represent the values for NaCl corresponding to the density profiles in Figures 1 (a) to (c). Similarly, open circles reflect the tension values for Na"F". In addition, experimental surface-tension values for NaCl are shown by the solid line in Figure 2, whereas the dashed line represents the surface-tension values for experimental NaF.[34] Clearly, both the salts show an increase in surface tension, and the MD results for NaCl solutions are quite close to the experimental values, suggesting that the

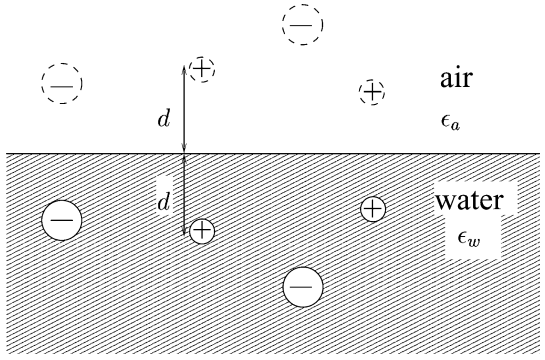

Figure 3. A schematic of the solvent primitive model (SPM) with water as a dielectric medium. The location of the interface is the discontinuity in the dielectric constant between water, ϵ_w, and air, ϵ_a. Both cations and anions are also shown schematically in the water region as solid circles, with their respective images in the air phase shown as dashed circles. The normal distance of one cation from the interface, *d*, is also highlighted.

potential models chosen for NaCl and H_2O are reasonable for predicting surface-tension values. Conistent with experiments, Na"F" (with a smaller anion) exhibits a larger increase in surface tension than does NaCl. Previous MD simulations by Daiguji and Hihara[35] (using SPC water and nonpolarizable ionic potentials for LiBr and KI) also show a similar trend where salts containing ions of smaller size (rather, smaller LJ σ and ϵ for ions) show a larger increase in surface tension than salts with larger ions. Results using polarizable potential models for both water and ions also show a similar trend.[31]

Primitive Model for Solvent

Using the same ionic-potential models as those in the explicit simulations, we calculate surface tensions for salt solutions in a primitive model where the solvent is treated as a dielectric continuum. This exercise gages the validity of a solvent primitive model. To establish the exact results for surface tension within the SPM framework, we adopt MD simulations. In SPM, water is a dielectric medium with a relative dielectric constant, ϵ_w, of 78.2. Accordingly, the coulombic part of the interaction between ions is reduced by a factor of ϵ_w. Because the ionic and water potential models in the explicit water simulations are not affected by the surroundings, we choose unchanged nonelectrostatic contributions (LJ) to the ion−ion interactions. Because the water is surrounded by vapor (or a medium of dielectric continuum of unity), a dielectric discontinuity is introduced at the interface that distorts the electrostatic potential from its value in bulk water. This distortion is usually modeled by introducing image charges.[36] Figure 3 depicts cations and anions (solid circles) near a water/air interface with dielectric discontinuity from ϵ_w to ϵ_a (the relative dielectric constant of air). The image of each ion is also shown as a dashed circle. A given ion in the solution interacts with all image charges.

As mentioned in the Introduction, another interaction that is usually considered when an ion is in the vicinity of the interface is the so-called dispersion interaction, measuring the extent to which the ions prefer to be in the bulk rather than near the interface or vice versa.[4,5] For our model of ions and the LJ model for nonelectrostatic interaction between ions and water, the ion-surface dispersion interaction results from integrating the r^{-6} part of LJ energy between the ion and the continuum of water taking into account the presence of interface (e.g., at a distance *d* for the labeled cation in Figure 3) and subtracting this from a similar value obtained when the ion is in bulk water. The

resulting expression is[4,5]

$$u_{\mathrm{i,vdw}} = \frac{B_{\mathrm{i}}}{d^3} \tag{3}$$

where B_{i} is a constant depending upon the type of ion, i. We discuss the particular choice of B_{i} shortly.

Since water is treated as a dielectric continuum, eq 2 for the surface tension is no longer appropriate. Thus, to calculate the change in surface tension due to the presence of ions, we use the Gibbs adsorption equation at constant temperature, or[8]

$$\mathrm{d}\gamma = -\sum_i \Gamma_{\mathrm{i(w)}}\, \mathrm{d}\mu_{\mathrm{i}} \tag{4}$$

where $\Gamma_{\mathrm{i(w)}}$ is the excess adsorption of ion species i at the location of the Gibbs interface defined by zero excess adsorption of water, and μ_{i} is the chemical potential of ionic species i. Due to overall electroneutrality of the solution, and the fact that both the cation and the anion density in the bulk must be the same for the 1:1 electrolytes, $\Gamma_{+(\mathrm{w})} = \Gamma_{-(\mathrm{w})} \equiv \Gamma$. Thus, upon introducing the salt chemical potential, $\mu = (\mu_+ + \mu_-)$, we rewrite eq 4 as

$$\mathrm{d}\gamma = -\Gamma\, \mathrm{d}\mu \quad \text{constant } T \tag{5}$$

which is valid for 1:1 electrolytes. Integration of eq 5 from the reference value (pure water) to a given μ (or, concentration) gives $\gamma - \gamma_{\mathrm{w}}$ as a function of concentration. Of course, eq 5 remains valid for the explicit water simulations as well, but direct evaluation of γ from eq 2 is expeditious.

Simulation Details. We again choose a slab geometry for our simulations of the solvent primitive model. A symmetric region of 4 nm thickness (in the *z* direction) having the dielectric constant of water is demarcated in the simulation box (of size 3.65 nm by 3.65 nm by 10 nm, as before). Thus, there is a vapor space (with $\epsilon_{\mathrm{a}} = 1$) outside the water dielectric continuum. Ions are placed in the region of dielectric water; the Ewald 3DC method of Yeh and Berkowitz[37] is invoked to account for the long-range forces between the ions. As mentioned before, distortion of the electrostatic potential due to the presence of the interface is treated via image charges. In our simulation system, the presence of two parallel interfaces implies that interaction with an infinite number of images for each ion must be considered.[38,39] However, we use a cutoff of 1 nm on the interionic potential when calculating the image charges. This limits the number of images considered considerably. We also used a larger cutoff of 1.5 nm and found that the large cutoff on the potential due to image charges introduced only a small difference (less than 5% for the lowest simulated concentration; at higher concentrations the effect is even smaller due to screening). We mention that a given instantaneous configuration of ions in the ensemble of configurations can be such that an ion is attracted to the interface by the image-charge forces.

For the dispersion potential, the expression for B_{i} in eq 3 is

$$B_{\mathrm{i}} = \frac{2\pi}{3}(\epsilon_{i,\mathrm{w}}\sigma_{i,\mathrm{w}}{}^6\rho_w - \epsilon_{i,\mathrm{a}}\sigma_{i,\mathrm{a}}{}^6\rho_{\mathrm{a}}) \tag{6}$$

where $\epsilon_{i,j}$ and $\sigma_{i,j}$ are the LJ parameters between molecules *i* and *j*, and the subscripts w and a refer to water (the oxygen in water) and the space above the water dielectric, respectively. Additionally, we make the assumption that the vapor space above the dielectric is empty ($\rho_{\mathrm{a}} \approx 0$). Note in eq 6 that the expression for B_{i} excludes an additional term due to the displacement of an equivalent amount of water from the interface to the bulk as an ion approaches the interface from the bulk. Since water is treated as a background dielectric continuum, we do not impart any graininess to water at any level. Moreover, as we show later, inclusion of such an additional term does not alter the qualitative nature of the results obtained. Column 2 of Table 1 lists the B_{i} values reduced by *kT*, where *k* is the Boltzmann constant, for the three types of ions calculated using eq 6.

TABLE 1: Coefficients Used in SPM

ion	B_{i}/kT (nm^3) (eq 6)	α_{i}/kT (nm^9)	B_{i}/kT (nm^3) (eq 7)
Na^+	4.75×10^{-3}	8.33×10^{-6}	-5.19×10^{-3}
Cl^-	3.30×10^{-2}	3.25×10^{-4}	-2.42×10^{-2}
F^-	1.21×10^{-2}	6.60×10^{-5}	-2.45×10^{-2}

In addition, our simulations with explicit water demonstrate that ions are repelled from the interface. With this physical picture, and to prevent ions from approaching the region of dielectric discontinuity too closely, we include a steep repulsive potential for ions approaching the sharp interface. This steep repulsive potential varies as the inverse-ninth power of the distance from the interface with the constants of proportionality, α_{i} reduced by *kT*, given in Column 3 of Table 1 for the three types of ions considered here. The inverse-ninth power is chosen because it represents the integrated repulsion of all the molecules of a wall with an approaching molecule, where the individual molecules repel each other by an inverse-twelfth power law. α_{Na^+} is set empirically to the value given in Table 1. All other α_{i} values are calculated using α_{Na^+} and the observation that the scaling constant in the inverse-ninth power law varies as $\epsilon_{i,\mathrm{w}}\sigma_{i,\mathrm{w}}$.[12] As we argue later, the range of values of α_{i} shown in Table 1 does not affect the surface tension results appreciably. Adoption of a steep repulsive potential is somewhat analogous to the use of different starting points for the solution of MPB equation.[4]

We simulate a range of salt concentrations and calculate the surface excess adsorption from the density profiles and individual ionic chemical potentials using the charge-scaling method of Svensson and Woodward.[40] Subsequently, we numerically integrate eq 5 to calculate the change in surface tension as a function of salt concentration.

Results for the SPM. First, we show the ionic density profiles for the minimum and the maximum concentrations simulated in the SPM for NaCl in Figures 4 (a) and (b), and for Na"F" in Figures 4 (c) and (d) at 300 K. In each figure, the solid line depicts the cation density profile, and the dashed line reports the anion density profile. The interface is at $z = 2$ nm for each figure. For both salts, as the concentration is increased, the difference between the cation and anion density profiles is magnified in the solvent primitive model. In contrast, at similar concentrations Figures 1 (a) and (c) show that when water is treated explicitly the difference is small for the same ionic-potential models. Additionally, the higher peak in the similar concentration anion density profiles in Figure 4 (b) and (d) is due the higher value of α_{Cl^-} than α_{F^-}. We return to this point shortly.

From the SPM density profiles, the surface excess adsorption, Γ, is calculated and plotted against the nondimensional chemical potential, $\beta\mu$ (where $\beta = 1/kT$), in Figure 5 for both NaCl (filled circles) and Na"F" (open circles). The lowest and the highest concentrations plotted in Figure 5 for both salts correspond to the density profiles shown in Figure 4. Even though the Cl^- density profile has a higher peak than the F^- density profile (compare Figures 4 (c) and (d)), Γ is the same for both Cl^- and F^- at the almost equal highest concentration simulated. Thus, the difference in the α_{i} values of the two anions in Table 1 has

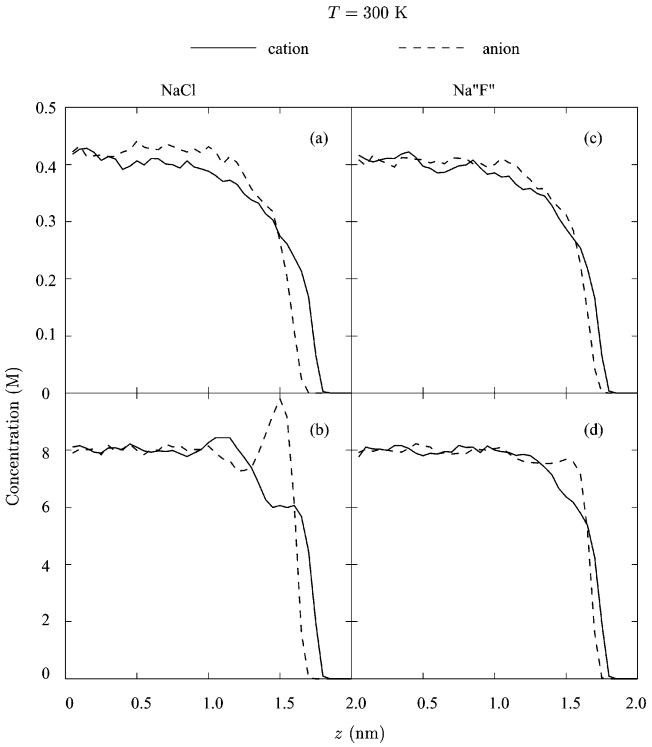

Figure 4. Ionic density profiles for the lowest and the highest simulated concentrations of NaCl ((a) and (b), respectively), and also of Na"F" in (c) and (d) in the SPM. The step interface is at $z = 2$ nm.

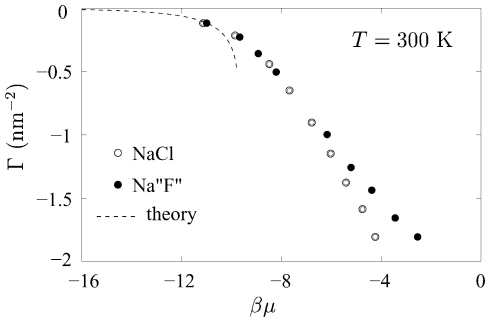

Figure 5. Surface excess adsorption of NaCl (filled circles) and Na"F" (open circles) as a function of the salt chemical potential in the SPM. The dashed theory line is an extrapolation to low concentrations.

only a small effect on the surface excess adsorption amounts. Since the lowest concentration we simulate is about 0.4 M for each salt, a method is needed to estimate the low-concentration tail of the $\Gamma-\mu$ plot which is needed to calculate the surface-tension by integration of eq 5. Such an extrapolation to $\mu = -\infty$ is depicted by the dashed line labeled in Figure 5 as "theory" and is described in Appendix A.

As is clear from Figure 5, the difference between the $\Gamma-\mu$ isotherms of the two salts progressively diminishes as the salt concentration decreases. This is expected because, at low solute concentrations, the solution approaches ideal-dilute behavior. For example, the chemical potential of a particular salt follows Henry's law with the Henry's constant dependent on the type of solute. However, since electrostatics dominates the interionic potentials, Henry's constant is approximately the same for both NaCl and Na"F". Thus, at any given low concentration, μ is approximately the same for both NaCl and Na"F". A similar argument also holds for the adsorption behavior at low concentrations (i.e., Γ is approximately the same for both NaCl and Na"F" for a given low enough concentration). In view of this, and the experimental fact that the difference between

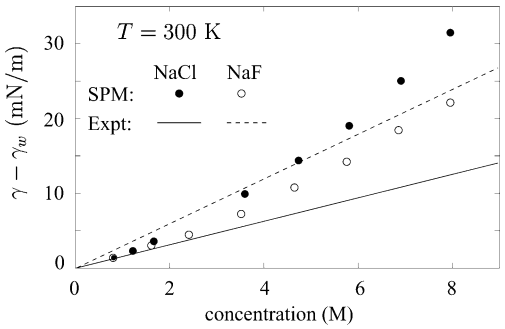

Figure 6. Surface tension of water relative to the surface tension of pure water as a function of salt concentration for the solvent primitive model for both NaCl and Na"F". Experimental values for both Na"F" and NaCl from Figure 2 are also depicted.

tension increases at high concentration of different salts is much more significant than such a difference at low concentrations, we use only one "theory" curve to extrapolate the $\Gamma-\mu$ plot of Figure 5 to zero salt concentration.

The chemical potential in Figure 5 includes the ideal-gas part and the explicit interactions between ions, but excludes the interaction between water and ions. In the solvent primitive model, the interaction between the continuum water and an ion is a unique constant for each type of ion that can be calculated analytically. Thus, if the continuum water-ion interaction is included, the points in Figure 5 shift on the μ scale by a different constant for each salt. But the value of the integral in eq 5 between the lowest and any other simulated concentration remains unchanged (for that particular salt). Moreover, the difference in the surface-tension increase over that of pure water between the lowest simulated concentration (almost identical) for either salt is not of particular importance in comparison to the much larger difference expected at higher concentrations (γ for 0.4 M NaCl is about 0.7 mN/m, whereas for 0.4 M Na"F" the value is 1.2 M). Thus, we define μ as used in Figure 5.

With eq 5 and using the data in Figure 5, we calculate the increase in surface tensions of both NaCl (closed circles) and Na"F" (open circles) in Figure 6 as a function of salt concentration for the SPM. Experimental results are repeated from Figure 2. Comparison of the MD results with explicit water in Figure 2 (i.e., the same as the experimental lines in Figure 6) and the SPM results in Figure 6 for the same ionic potentials shows qualitative differences. For explicit water, Na"F" (with a smaller anion) exhibits a larger increase in surface tension than does NaCl (with a larger anion), in agreement with experiments. For the primitive water, this trend is reversed. Thus, even a rigorous calculation of the surface-tension change in the primitive model for solvent fails to explain qualitatively the effect of the type of salt on the surface tension. Said in another way, the SPM reverses the order of the Hofmeister series.

In Figure 6, the values of B_i (see eq 5) do not account for the dispersion component of the so-called equivalent volume of water.[4] This correction modifies eq 6 to

$$B_i = \frac{2\pi\rho_w}{3}\left[\epsilon_{i,w}\sigma_{i,w}{}^6 - \left(\frac{\sigma_i}{\sigma_w}\right)^3 \epsilon_{w,w}\sigma_{w,w}{}^6\right] \qquad (7)$$

where $(\sigma_i/\sigma_w)^3$ represents the equivalent volume of water. In eq 7, we neglect the term proportional to ρ_a in eq 6 as it is negligible in comparison. Equation 7 yields negative values for all B_i coefficients given in Column 4 of Table 1. In addition, the difference between B_{Cl}/kT and B_F/kT is now rather small. Figure 7 graphs the density profiles of Cl^- using B_{Cl^-} calculated from eq 6 (dashed line, also see Figure 4 (b)) and from eq 7

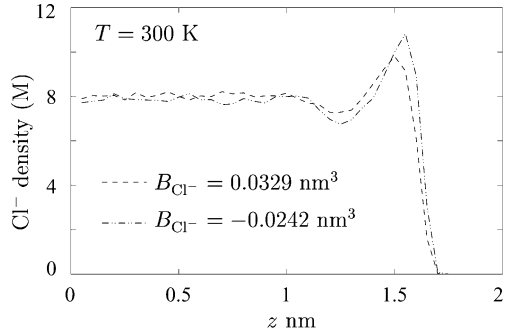

Figure 7. Density profiles for Cl^- in SPM obtained by not subtracting out the equivalent volume of water (dashed line, eq 6) and upon subtracting out such a term (dashed−dotted line, eq 7).

(dashed−dotted line) for the same total number of ions in the system. Evidently, even the change in sign of B_{Cl^-} does not affect the density profile, and hence, the surface-tension behavior (Figure 6). The reason for the insensitivity of the surface-tension results to the values of B_i in this range is because very near the interface the steeply repulsive inverse-ninth power dominates and determines the ion-density profile. Thus, even though the difference between α_i coefficients chosen for different ions have a negligible effect on the respective surface-tension values (as already mentioned), the presence of a short-range steeply repulsive potential is enough also to negate the effect of B_i coefficients (for the range of values chosen).

The main reason for the difference in surface-tension values in SPM is that the change in the chemical potential for each salt from its lowest to its highest simulated value is different (cf., Figure 5). And, this value is unaffected by changing B_i's. Presumably, if the value of B_{F^-} is chosen empirically to be much larger than that for B_{Cl^-} so that Γ for Na"F" at the same concentration is significantly more negative than that for NaCl (to offset the significantly larger increase in the chemical potential for NaCl), the surface-tension curve for Na"F" may eventually rise above that for NaCl. Nevertheless, such a choice of B_{F^-} does not correspond to the potential model used in the explicit MD and becomes a fitting parameter.

Very recent calculations within the SPM using the MPB approach by Manciu and Ruckenstein[6] establish that inclusion of hydrated ion sizes (by employing different starting locations for the solution of MPB) can dominate the effect of B_i coefficients, in agreement with our findings. Thus, inclusion of the different hydrated ion sizes for different ions in SPM (e.g., by empirically varying α_i coefficients to a much larger range than in Table 1) can readily make the surface tension of Na"F" larger than that of NaCl.

Figure 5 also suggests a possible explanation of the results of Jungwirth and Tobias[31] that NaBr and NaI solutions at 1.2 M exhibit an increase in surface tension (over that of pure water) despite being positively adsorbed at that concentration. It is likely for certain ionic-potential models that Γ is initially negative, and then curves in Figure 5 to positive values at higher concentrations. Since the surface-tension increase over that of pure water at a particular concentration is the integral in eq 5 from zero salt concentration to the concentration of interest, $\gamma - \gamma_w$ may be positive even when Γ is positive for that concentration. This reasoning implies a maximum in the surface tension-versus-concentration isotherm. Unfortunately, Jungwirth and Tobias did not investigate a range of electrolyte concentrations. Further, the experimental data for the surface tension of NaBr or NaI aqueous solutions do not exhibit a maximum.

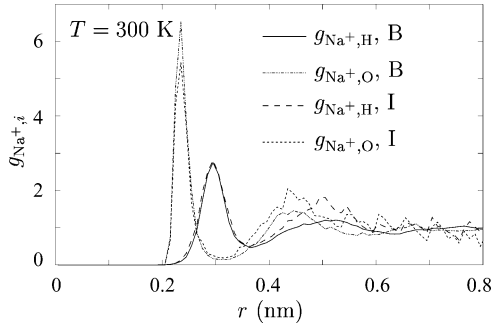

Figure 8. Pair-correlation functions of the O and H atoms of water from a central sodium ion in the bulk and near the interface for the system in Figure 1 (f).

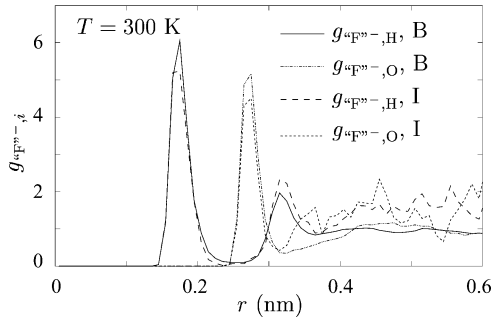

Figure 9. Pair-correlation functions of the O and H atoms of water from a central chloride ion in the bulk and near the interface for the system in Figure 1 (f).

Role of Water Structure around Ions

Since for MD simulations with explicit water molecules the surface-tension trend for halide salts is same as that in experiment, a primary reason for the opposite surface-tension trend for halide salts predicted by the SPM is the treatment of water as a dielectric continuum. In fact, previous molecular simulations show that water is highly structured around bulk ions.[9−11] The oxygen of water is nearest to a cation, and the hydrogens of water are oriented such that the dipole of water is pointed directly outward from a cation. For anions, one of the hydrogen−oxygen bonds of water lies along the radial position of the anion with the hydrogen closer to the anion. Moreover, as the ion size increases, the orientational structure becomes more diffuse.

Figures 8 and 9 graph the pair correlation function of the oxygen and hydrogen atoms of water around a central cation and a central anion, respectively, for Na"F" at the highest concentration simulated with explicit water molecules (cf., Figure 1 (f)). In both figures, the solid line represents the pair correlation function of hydrogen atoms of water around the ions in the bulk of the solution ($|z| \leq 0.1$ nm). Similarly, the dashed−dotted lines are for the oxygen atom of water molecules. The distance between the locations of the O and H peaks in Figures 8 and 9 reflects the structuring of water around ions, as mentioned above. Additionally, we show the pair correlation function of H (long-dashed line) and O (short-dashed line) around the cations (Figure 8) and anions (Figure 9) when the ions are near the interface (1.5 nm $\leq z \leq$ 1.7 nm in Figure 1 (f), and the symmetric negative position). In the case of ions near the interface, the pair correlation function is evaluated along the direction normal to the interface (i.e., the angle between the radially outward direction from the ion and the direction normal to the interface, the z axis, is between 0 and $\pi/10$).

Figures 8 and 9 reveal that the ions retain the first shell of water molecules (defined by the first O and the corresponding

two H peaks) in the exact same configuration as in the bulk for Na"F". Insufficient sampling near the interface precludes any such observation beyond the first shell. Thus, not only are the simulated ions repelled from the interface (cf., Figure 1), the water structure in the immediate vicinity of the ions is same as in the bulk as well. Even at any other angular orientation (apart from between 0 and $\pi/10$ as mentioned above), the structure of water around ions is the same as shown in Figures 8 and 9, further supporting the fact that the presence of the interface does not distort the structure of water around ions. For the NaCl potential model, we again observe the same behavior both in bulk and near the interface (with the orientation around the larger Cl^- more diffuse both in the bulk[9−11] as mentioned above and also near interface).

Comparison of Figures 1 (a) and (d) suggests that at similar concentrations, Na"F" (smaller anion) is more repelled from the interface than NaCl. A stronger orientation of water around the smaller halide ion is, perhaps, responsible for the salt containing Na"F" being repelled more from the interface. This observation can be related to the difference in the sizes of hydrated ions. Since this difference in bulk structure of high-density water around ions of different sizes depends mainly on ion sizes and not appreciably on the dispersion interactions between ions and water, it is not possible to explain ion specificity solely on the basis of dispersion interactions manifested through the B_i coefficients as is currently done in SPM.

Conclusions

We perform MD simulations of electrolytic solutions to study the specific-ion effect on the surface tension. First, explicit water with ions is simulated. The chosen potential models for ions are such that two different salts with different anion sizes, NaCl and Na"F", are represented. We find that the ionic and water potential models chosen give a good representation of the surface-tension properties of NaCl. In particular, Na"F" solutions (with a smaller anion) show a higher increase in surface tension than do NaCl solutions. Also, we find that ions are preferentially repelled from the interface for the given potential models, and they retain, at least, their first hydrated water shell, as in the bulk. With the explicit-water simulations, we obtain a benchmark against which theories using the same ionic-potential models can be checked.

Next, we solve exactly the model with water as a dielectric continuum using MD simulations to obtain the best results that are possible within the SPM. In this exercise, we use the same ionic-potential models as in the explicit water case. Even the exact solution of SPM gives results for surface tension that are qualitatively different from that for explicit water. SPM predicts that solutions of NaCl (with a larger anion) show a larger increase in surface tension than do solutions of Na"F". The discrepancy between SPM and explicit water results is most likely due to the fact that in SPM the difference solvation behavior of different ions (e.g., the different structure of water around different sizes of anions), that is present even near the interface, is not taken into account.

Appendix A: Extrapolation of $\Gamma-\mu$ Isotherm to Low Concentration

Our method of extrapolation of the $\Gamma-\mu$ plot (the theory line in Figure 5) is based on the Onsager-Samaras method.[2] In addition to pure electrostatics considered by Onsager and Samaras, we include the ion-surface dispersion interaction between the interface and ions. To avoid charge separation, and the subsequent creation of an electrostatic potential, the same B_i is used for all the ions. This is not a crucial step because the change in surface tension from zero to the lowest simulated salt concentration in SPM is expected to be small, as mentioned in the text, and also due to the fact that the results are expected to be insensitive to the B_i coefficients at low concentrations. Thus, the total amount adsorbed is calculated by quadrature from

$$\Gamma = c_b \int_0^\infty \left(\exp\left[-\left(\frac{e^{\kappa a}}{1+\kappa a}\right)\left(\frac{{q_e}^2}{16\pi\epsilon_0\epsilon_w kT}\right) \times \left(\frac{\epsilon_w-\epsilon_a}{\epsilon_w+\epsilon_a}\right)\frac{e^{-2\kappa z}}{z} - \frac{B_i}{z^3}\right] - 1 \right) dz \quad \text{(A1)}$$

where c_b is the bulk electrolyte concentration, κ is the reciprocal Debye length calculated in the bulk, q_e is the electronic charge, z is the distance from the interface (at $z = 0$) toward the bulk of the electrolyte solution (at $z = \infty$), and a is a parameter describing the ionic size. As for B_i, a is also chosen to be a unique number for the purpose of the extrapolation. Instead of assigning a rigorous physical meaning to B_i/kT ($= 0.032$ nm^3) and a ($= 0.22$ nm), we treat them as fitting parameters to match the "theory" curve in Figure 5 with the results from SPM simulations at the lowest concentration. The excess (over the ideal-gas part, $kT \ln c_b$) chemical potential is obtained by the Debye−Huckel expression. Combining μ thus obtained with Γ from eq A1 gives the "theory" curve in Figure 5.

References and Notes

(1) Washburn, E. W. *International Critical Tables of Numerical Data. Physics, Chemistry, and Technology*; McGraw-Hill: New York, 1928; Vol. IV.
(2) Onsager, L.; Samaras, N. N. T. *J. Chem. Phys.* **1934**, *2*, 528.
(3) Bhuiyan, L. B.; Bratko, D.; Outhwaite, C. W. *J. Phys. Chem.* **1991**, *95*, 336.
(4) Bostrom, M.; Williams, D. R. M.; Ninham, B. W. *Langmuir* **2001**, *17*, 4475.
(5) Karraker, K. A.; Radke, C. J. *Adv. Colloid Interface Sci.* **2002**, *96*, 231.
(6) Manciu, M.; Ruckenstein, E. *Adv. Colloid Interface Sci.* **2003**, *105*, 63.
(7) Collins, K. D.; Washabaugh, M. W. *Q. Rev. Biophys.* **1985**, *18*, 323.
(8) Newman, J. *Electrochemical Systems*; Prentice Hall: New York, 1991; Chapter 7.
(9) Hummer, G.; Pratt, L. R.; Garcia, A. E. *J. Phys. Chem.* **1996**, *100*, 1206.
(10) Garde, S.; Hummer, G.; Paulaitis, M. E. *J. Chem. Phys.* **1998**, *108*, 1552.
(11) Heinzinger, K.; Bopp, P.; Jancso, G. *Acta Chim. Hung.* **1985**, *121*, 27.
(12) Schafer, K.; Masia, A. P.; Juntgen, H. *Z. Elektrochem.* **1955**, *59*, 425.
(13) Wagman, D. *J. Phys. Chem. Ref. Data* **1982**, *11* (supplement 2).
(14) Berendsen, H. J. C.; Grigera, J. R.; Straatsma, T. P. *J. Phys. Chem.* **1987**, *91*, 6269.
(15) Wheeler, D. R. Ph.D. Dissertation, University of California, Berkeley, 2002.
(16) Heinzinger, K. *Physica* **1985**, *131B*, 196.
(17) Nose, S. *Mol. Phys.* **1984**, *52*, 255.
(18) Hoover, W. G. *Phys. Rev. A* **1985**, *31*, 1695.
(19) Frenkel, D.; Smit, B. *Understanding Molecular Simulations*; Academic Press: New York, 1991; Chapter 6.
(20) Allen, M. P.; Tildesley, D. J. *Computer Simulation of Liquids*; Clarendon Press: Oxford, 1987; Chapter 7.
(21) de Leeuw, S. W.; Perram, J. W.; Smith, E. R. *Proc. R. Soc. London, Ser. A* **1980**, *373*, 27.
(22) Karasawa, N.; Goddard, W. A. *J. Phys. Chem.* **1989**, *93*, 7320.
(23) Wheeler, D. R.; Rowley, R. L. *Mol. Phys.* **1998**, *94*, 555.
(24) Bhatt, D.; Newman, J.; Radke, C. J. *J. Phys. Chem. B* **2003**, *107*, 13076.
(25) Alejandre, J.; Tildesley, D. J.; Chapela, G. A. *J. Chem. Phys.* **1995**, *102*, 4574.
(26) Irving, J. H.; Kirkwood, J. G. *J. Chem. Phys.* **1950**, *18*, 817.
(27) Walton, J. P. R. B.; Tildesley, D. J.; Rowlinson, J. S. *Mol. Phys.* **1983**, *48*, 1357.
(28) Nose, S.; Klein, M. L. *Mol. Phys.* **1983**, *50*, 1055.

(29) Huang, D. M.; Geissler, P. L.; Chandler, D. *J. Phys. Chem. B* **2001**, *105*, 6704.
(30) Kalra, A.; Tugcu, N.; Cramer, S. M.; Garde, S. *J. Phys. Chem. B* **2001**, *105*, 6380.
(31) Jungwirth, P.; Tobias, D. J. *J. Phys. Chem. B* **2001**, *105*, 10468.
(32) Wilson, M. A.; Pohorille, A.; Pratt, L. R. *Chem. Phys.* **1989**, *129*, 209.
(33) Marrink, S.-J.; Marcelja, S. *Langmuir* **2001**, *17*, 7929.
(34) For NaCl, the experimental results are up to a concentration of 6 M; the line between 6 and 8 M is an extrapolation. Moreover, the experimental NaCl results are at 293 K. However, $\gamma - \gamma_w$ is independent of temperature for at least up to 303 K.[1] For NaF, experimental results are available up to only about 0.5 M; the dashed line is mainly an extrapolation. Moreover, as mentioned in the Introduction, any comparison between MD specific Na"F" solution and experimental NaF solution is not to be taken quantitatively.
(35) Daiguji, H.; Hihara, E. *Heat Mass Transfer* **1999**, *35*, 213.
(36) Jackson, J. D. *Classical Electrodynamics*; John Wiley and Sons: New York, 1999; Chapter 4.
(37) Yeh, I.-C.; Berkowitz, M. L. *J. Chem. Phys.* **1999**, *111*, 3155.
(38) de Leeuw, S. W.; Perram, J. W. *Mol. Phys.* **1979**, *37*, 1313.
(39) Yang, P.-K.; Liaw, S.-H.; Lim, C. *J. Phys. Chem. B* **2002**, *106*, 2973.
(40) Svensson, B. R.; Woodward, C. E. *Mol. Phys.* **1988**, *64*, 247.